Climate Dynamics (2018) 51:2707–2723
https://doi.org/10.1007/s00382-017-4038-6

Synoptic characteristics, atmospheric controls, and long-term changes of heat waves over the Indochina Peninsula

Ming Luo[1,2] · **Ngar-Cheung Lau**[1,3]

Received: 3 May 2017 / Accepted: 4 December 2017 / Published online: 11 December 2017

Abstract
The characteristics of heat wave (HW) events over the Indochina Peninsula are studied using the Climate Forecast System Reanalysis data for 1979–2010. HWs in the dry and wet seasons of Indochina are considered separately, and their typical synoptic behavior is examined in detail. Our results show that HWs in both seasons are accompanied by suppressed precipitation, and the region lies under an anomalously dry, hot, and subsiding atmospheric column. Further diagnoses reveal that HWs in the dry and wet seasons are linked to the weakening of the East Asian winter monsoon (EAWM) and the South Asian summer monsoon (SASM) circulations, respectively. On the one hand, HWs in the dry season are coincident with high-temperature anomalies over East Asia and accompanied by an anomalous cyclone over eastern China. The anomalous southwesterly flow over East Asia indicates a weakening of the climatological northeasterly circulation associated with the EAWM. On the other hand, HWs in the wet season are coincident with hot and dry anomalies in South Asia (i.e., Indian subcontinent). The anomalous easterly flow in that region opposes the climatological westerly regime of the SASM. Moreover, we found that the statistics for the frequency, duration, and amplitude of HWs for both seasons exhibit prominent intensifying trends, and the intensifying trends in the wet season are mostly about two to three times stronger than the dry season. These intensifying HWs activities are likely attributable to the weakening trend of monsoon circulations in recent decades.

Keywords Heat waves · Indochina Peninsula · Synoptic characteristics · East Asian winter monsoon · South Asian summer monsoon · Climate change

1 Introduction

Heat waves (HWs) have serious impacts on human health and can even cause human deaths (IPCC 2012; Meehl and Tebaldi 2004). For instance, the European HW event in 2003 caused more than 70, 000 deaths (Robine et al. 2008). A study on the risk of HWs on mortality in 43 US cities shows that mortality increases by 3.73% during HW days as compared with non-HW days (Anderson and Bell 2011). Besides human health, HWs can also lead to other complex social issues, such as increasing psychological stress and violent crimes (Simister and Cooper 2005), as well as incidence of power outages, wildfires, and damage to infrastructures (Zuo et al. 2015).

With global warming, the frequency and intensity of HWs have been projected to increase in the future and may pose more severe threats to society (Christidis et al. 2015; Meehl and Tebaldi 2004). The change of HWs is in accord with the global warming trend and human activity has a significant influence on the increasing severity of hot events (Christidis et al. 2011; Coumou and Rahmstorf 2012).

In addition to the long-term change of HWs, previous investigations have been devoted to studying their synoptic features and physical causes. For instance, Loikith and Broccoli (2012) found that high-temperature extremes in most regions of North America are accompanied by positive 500-mb geopotential height anomalies, and positive downstream and negative upstream perturbations in surface pressure. A

✉ Ming Luo
luo.ming@hotmail.com

[1] Institute of Environment, Energy and Sustainability, The Chinese University of Hong Kong, Sha Tin, N.T., Hong Kong

[2] Guangdong Key Laboratory for Urbanization and Geo-simulation, School of Geography and Planning, Sun Yat-sen University, Guangzhou 510275, China

[3] Department of Geography and Resource Management, The Chinese University of Hong Kong, Sha Tin, N.T., Hong Kong

persistent and quasi-stationary high-pressure synoptic system in the mid-latitudes, known as atmospheric blocking, is an important contributing factor for HWs (Dole et al. 2011; Matsueda 2011; Sillmann and Croci-Maspoli 2009). Up to 80% of hot extremes in northern Europe, for example, are associated with the blocking (Pfahl and Wernli 2012). The atmospheric blocking alters the path of mid-latitude jets, prevents the propagation of synoptic weather systems, and favors the warm temperature extremes due to adiabatic warming and clear-sky radiative heating (Brunner et al. 2017; Pfahl and Wernli 2012; Pfahl et al. 2015). HWs in East Asia are found to be associated with the westward extension of the western North Pacific subtropical high (Ding et al. 2010; Luo and Lau 2017) and the displacement of the East Asian jet stream (EAJS) (Wang et al. 2013, 2016). Hot extremes are also linked to circulations such as the North Atlantic Oscillation (Guirguis et al. 2011), El Niño-Southern Oscillation (Hu et al. 2013; Kenyon and Hegerl 2008), Indian Ocean Dipole (White et al. 2014), and Indian Ocean basin mode (Hu et al. 2011; Huang et al. 2012). In addition to the atmospheric effects, HWs can be amplified by negative anomalies in soil moisture (García-Herrera et al. 2010; Miralles et al. 2014). More advances in the measurement, driving mechanisms, and the changes of HWs are summerzied by Perkins and Alexander (2013), Perkins (2015), Grotjahn et al. (2016), and You et al. (2017).

Previous studies have broadened our understanding of the contributory factors and processes underlying the development of HWs in various regions. However, there are relatively fewer investigations on HWs in developing tropical areas such as the Indochina Peninsula (also known as Mainland Southeast Asia). The Indochina Peninsula is situated between the Indian and Pacific Oceans (Fig. 1) and is comprised of six developing countries, namely, Cambodia, Laos, Malaysia, Myanmar, Thailand, and Vietnam. The economic development of this region lags behind the developed countries, and its basic infrastructures are more vulnerable to natural hazards, such as those brought about by climate change and weather extremes (Marks 2011).

The climate over the Indochina Peninsula is influenced by the monsoon subsystems in both East Asia and South Asia, and the atmospheric signals accompanying HW episodes in this region might be different from other regions. However, the behaviors of HWs in Indochina have not been studied extensively. It is, therefore, worthwhile to gain a comprehensive understanding of contributing factors and mechanisms of HWs in this region. Such investigation is also important for designing early warning information systems for extreme high temperatures.

This paper is organized as follows. Sect. 2 introduces the dataset and describes the procedure for identifying HWs in two distinct seasons of Indochina, namely, dry and wet seasons.Section 3 describes the evolution process of the HW development. Section 4 presents a comprehensive analysis on the synoptic behavior and large-scale atmospheric influences during HW occurrences. The long-term changes in various statistical measures of these HWs are then examined in Sect. 5. The principal findings are summarized and discussed in Sect. 6.

2 Datasets and methodology

2.1 Datasets

The primary dataset used in this study is the Climate Forecast System Reanalysis (CFSR) product generated by the National Centers for Environmental Prediction (NCEP). This product has a fine spatial resolution of 38 km, and its applicability for studying the details of various regional circulation systems has been demonstrated (Lau and Nath 2014). This reanalysis dataset covers the 1979–2010 period. More information on the data input and procedures used for generating the CFSR product are documented by Saha et al.

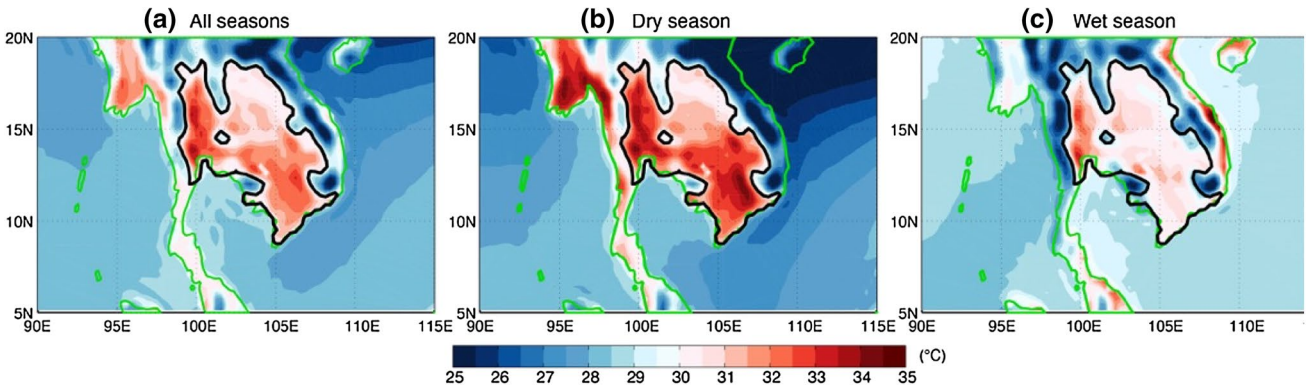

Fig. 1 Climatological mean daily maximum temperature (T_{max}) over the Indochina Peninsula in **a** all seasons, **b** dry season, and **c** wet season of 1979–2010. Black thick contour indicates the study region in central Indochina Peninsula with the annual mean T_{max} higher than 30 °C

(2010). The observed patterns presented in this study are obtained from daily grids of maximum near-surface temperature (T_{max}), specific humidity, sea level pressure (SLP), geopotential height, horizontal wind and pressure velocity.

In addition, the unified gauge-based analysis of global daily precipitation produced by NOAA Climate Prediction Center (CPC) is used to determine the monsoon onset and withdrawal dates over the Indochina Peninsula. This rainfall dataset is based on records at over 30,000 stations that were collected from multiple sources (Xie et al. 2007). The daily precipitation on a 0.5° latitude/longitude grid over the Indochina Peninsula is analyzed for the study period.

Daily anomalies are calculated by removing the climatological seasonal cycle, as obtained by computing the multi-year averages for individual calendar days and then performing a 31-day running mean, from the daily series for various years. In the composite analysis, an average is first taken over the duration of each HW event; then the average over all the events in the dry or wet season is taken (by giving equal weight to each event) to yield the composite values of anomalies.

2.2 Description of the study region

We define our study region as the central part of the Indochina Peninsula with the climatological annual mean T_{max} higher than 30 °C (Fig. 1). The climate in the Indochina Peninsula is characterized by two distinct seasons (separated by monsoon onset and withdrawal dates, see Sect. 2.3), with a dry season extending from November to April and a wet season from May to October (Fig. 2). In the dry season, low-level northeasterly winds prevail over the South China Sea (SCS), which is situated to the east of the peninsula (Fig. 3a). In the wet season, the circulation is dominated by southwesterly flow over the Bay of Bengal (BOB), which is associated with the South Asian summer monsoon (SASM). These monsoon winds transport moisture eastward and bring abundant rainfall to the peninsula (Fig. 3b).

As shown in Fig. 2, there is a remarkable temporal shift between the seasonal evolutions of T_{max} and precipitation. The temperature in the study region is lowest in the early and middle winter season, i.e., from November to January; whereas the highest temperature appears in late winter and spring season, i.e., from February to May, with the highest T_{max} exceeding 40 °C in many years. However, the rainy season of the study region begins in May and ends in October. The climatological mean onset date of the wet season (see definition in the following subsection) is May 10, while the climatological end date is October 16. This shift in the seasonal cycles of T_{max} and precipitation suggests that the role of moist atmospheric processes in the formation and development of HWs in the two seasons might be different. Moreover, the prevalent atmospheric circulations in the dry and wet seasons are rather distinct, and are linked to the East Asian summer monsoon (EAWM) and SASM, respectively. In view of these relationships, it is likely that the synoptic behavior and atmospheric controls of HWs in the dry and wet seasons are also different. The potential distinctions in synoptic features and ambient atmospheric environments of HWs in these two subperiods of the seasonal cycle are the main focus of the present study.

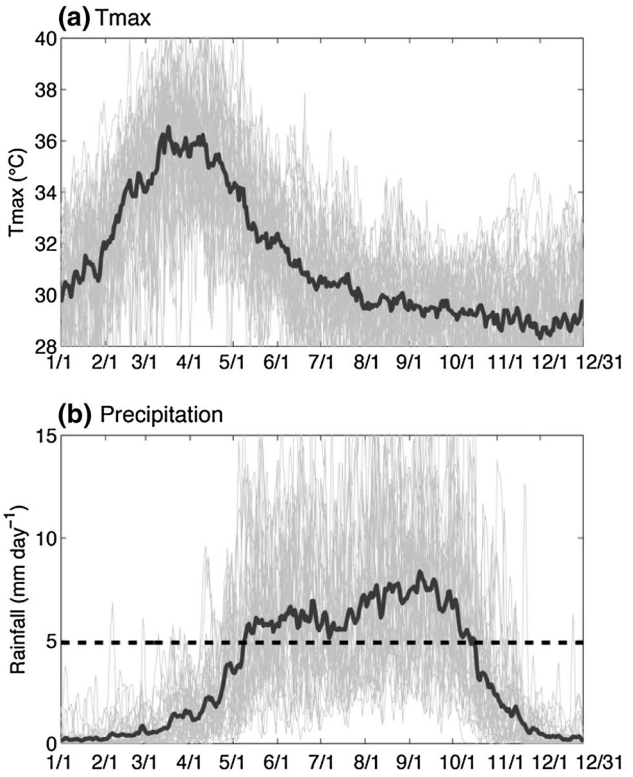

Fig. 2 The climatological seasonal cycle of daily **a** T_{max} and **b** precipitation averaged over the study region in Indochina during the 1979–2010 period (bold curves). Light curves indicate the seasonal cycles of individual years within this period. The horizontal line in the bottom panel shows the threshold of 5 mm/day, which is used to determine the monsoon onset and withdrawal dates

2.3 Determination of dry and wet seasons

HW events are independently identified for the dry and wet seasons. In this study, dry and wet seasons in a given year are separated by the onset and withdrawal dates of the rainy season over the region. The wet season refers to the period spanning from the onset date of the rainy season to the withdrawal date, while the dry season is defined as the remainder. To determine the monsoon onset and withdrawal dates, we adopt the methodology proposed by Zhang et al. (2002), who defined the monsoon onset date as the day when: (1) the amount of the daily precipitation rate exceeds 5 mm per day and persists continuously for 5 days; (2) within the 20-day

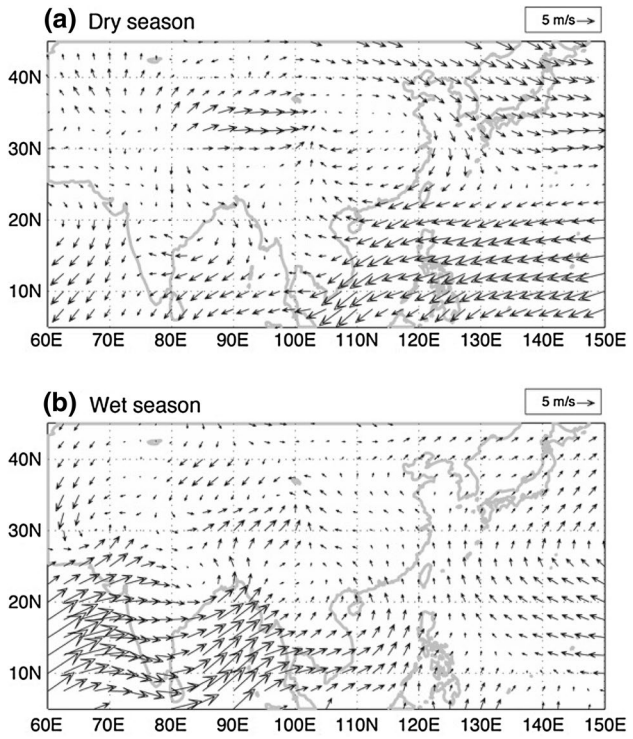

Fig. 3 Climatological mean 925-mb wind over South and East Asia in the dry (upper panel) and wet (lower panel) seasons of 1979–2010

period after the onset, more than 10 days receive rainfall amounts of 5 mm per day or more.

However, Zhang et al. (2002) did not provide a definition for the monsoon withdrawal. By examining the seasonal cycle of precipitation (Fig. 2b), we notice that it exhibits an abrupt decrease around the mid-October. This evolution is the reverse of that associated with the monsoon onset and is indicative of monsoon withdrawal. We thus define the monsoon withdrawal date as the day when: (1) the amount of the daily precipitation rate drops to less than 5 mm per day and persists at that dry level continuously for 5 days; (2) within the 20-day period after the withdrawal, more than 10 days receive rainfall amounts of less than 5 mm per day. Using the above definitions, yearly monsoon onset and withdrawal dates over the study region are identified.

2.4 HW identification and measures

After determining the monsoon onset and withdrawal dates of each year, HW events are then identified separately for the wet and dry seasons, based on daily time series of the spatial average of T_{max} over the study region. Following previous studies (Lau and Nath 2014; Luo and Lau 2017), a regional HW event is defined when the regional mean daily T_{max} satisfies the following three criteria:

a. T_{max} must be higher than the 90th percentile value of T_{max} for all available years (hereafter referred to as T1) for three or more consecutive days;
b. averaged T_{max} over the entire event must exceed T1 ;
c. T_{max} on each day of the event must be higher than the 75th percentile value of T_{max} for all available years (hereafter referred to as T2).

To examine the long-term trends of various aspects of HW activities, we focus on the HW measures including (Table 1): the yearly number of HW events (HWN), yearly sum of participating HW days (HWF), length of the longest yearly event (HWD), maximum temperature of the hottest day of the hottest yearly event (i.e., amplitude, HWA), average length of all yearly events (HWL), average magnitude of all yearly events (HWM), onset date of the first event of the year (HWO), and ending date of the last event of the year (HWE). Here, the onset (ending) date is defined as the first (last) day with $T_{max} > T2$ during the HW event. The trends of these measures are estimated by a modified Mann–Kendall trend test that accounts for series autocorrelation, as described by (Hamed and Rao 1998).

Table 1 Definitions of heat wave (HW) measures and their differences between weak and strong monsoon years, i.e., weak minus strong EAWM (SASM) years for dry (wet) season

HW measures	Definition (unit)	Dry season	Wet season
Seasonal T_{max}	Mean T_{max} averaged throughout the season (°C)	+ **1.11**	+ **0.55**
HWN	Yearly number of HW events (event)	+ 0.20	+ **1.54**
HWF	Yearly sum of participating HW days (day)	+ **9.64**	+ **24.22**
HWD	Length of the longest yearly event (day)	+ **5.11**	+ **8.74**
HWA	Hottest day of the hottest yearly event (°C)	+ 0.18	+ 0.37
HWL	Average length of all yearly events (day)	+ **4.75**	+ **3.01**
HWM	Average magnitude of all yearly events (°C)	+ **0.07**	+ 0.01
HWO	Onset date of the first event of the year (day)	+ 4.55	+ **15.25**
HWE	Ending date of the last event of the year (day)	+ 15.57	+ **38.93**

Bold values denote significance at the 95% confidence level as obtained by t-test

3 Development of heat waves

By this definition, altogether 45 and 43 HW events are identified in dry and wet seasons, respectively. We now proceed to construct their composite patterns of T_{max} and low-level wind at 925-mb, to illustrate the development of HWs in Indochina and to unravel their possible controlling factors. Note that we choose 925-mb for displaying these patterns because the wind field at this level can clearly indicate the change of monsoon circulations (Chang 2004), and it is closely related to the surface warming associated with the HWs. The evolution of these anomalies at the incipient stage of HWs in the dry and wet season is depicted in Figs. 4 and 5, respectively. Composite charts are arranged at a 1-day interval for the temporal lags of −3 to 0 days versus the onset date. These patterns portray the temporal evolution of high T_{max} and low-level wind anomalies associated with HWs in the Indochina Peninsula.

Three days before the onset of HWs (day −3, see Fig. 4a), high-temperature anomalies appear in northern parts of East Asia. These anomalies intensify and extend southward with time (day −2 to day −1). They cover most parts of East Asia and reach the northeastern Indochina region on the day before HWs start (day −1). On the onset date of HWs in Indochina (day 0), high temperatures cover most parts of the Indochina Peninsula, with the highest temperature appearing in the northern part of that region. Meanwhile, high temperatures appear in many parts of East Asia, i.e., eastern China, the Korean Peninsula, and southern Japan.

This southward propagation of high-temperature anomalies from northern East Asia corresponds well with the southward extension of the anomalous southwesterly wind. Here, anomalous southwesterly wind indicates a weakening of the northeasterly EAWM circulation. These anomalous southwesterly low-level winds start from northern East Asia (day −3), and intensify and propagate southward to the SCS region (days −2 to −1). They cover the most parts of Indochina when HWs in Indochina commence (day 0). This simultaneous relationship between the propagations of high temperature anomalies and the weakening of EAWM imply that the change of the EAWM circulation may play a substantial role in the development of HWs in the dry season of Indochina. To further examine the possible association with the EAWM circulation, we calculate the composite

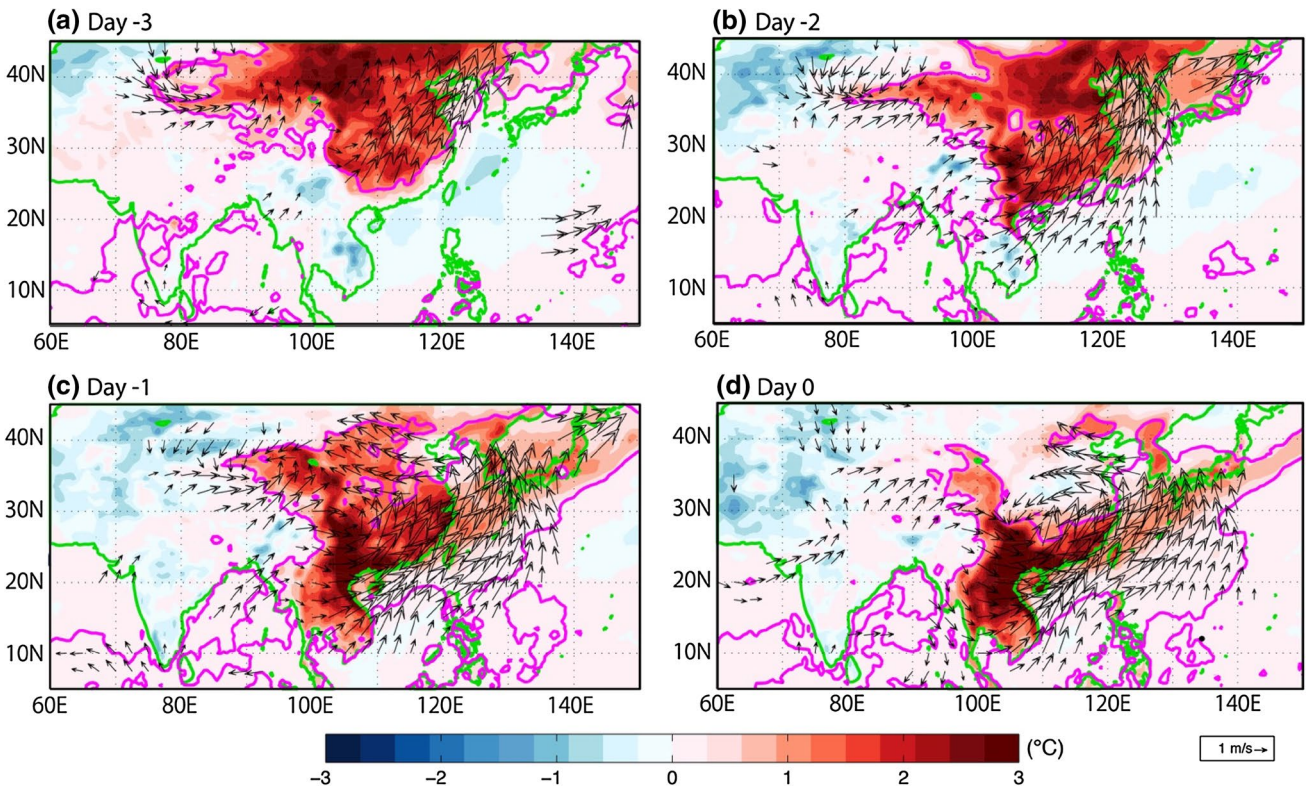

Fig. 4 Composite charts of the evolution of anomalous T_{max} (shading) and 925-mb wind (vector) prior to the occurrence of HW in the dry season. Day 0 denotes the onset day of the HW event. Day −1 denotes the day before Day 0, and so forth. Purple thick contour denotes significant positive T_{max} anomalies at the 95% confidence level, and significant wind anomalies either for zonal or meridional components are plotted

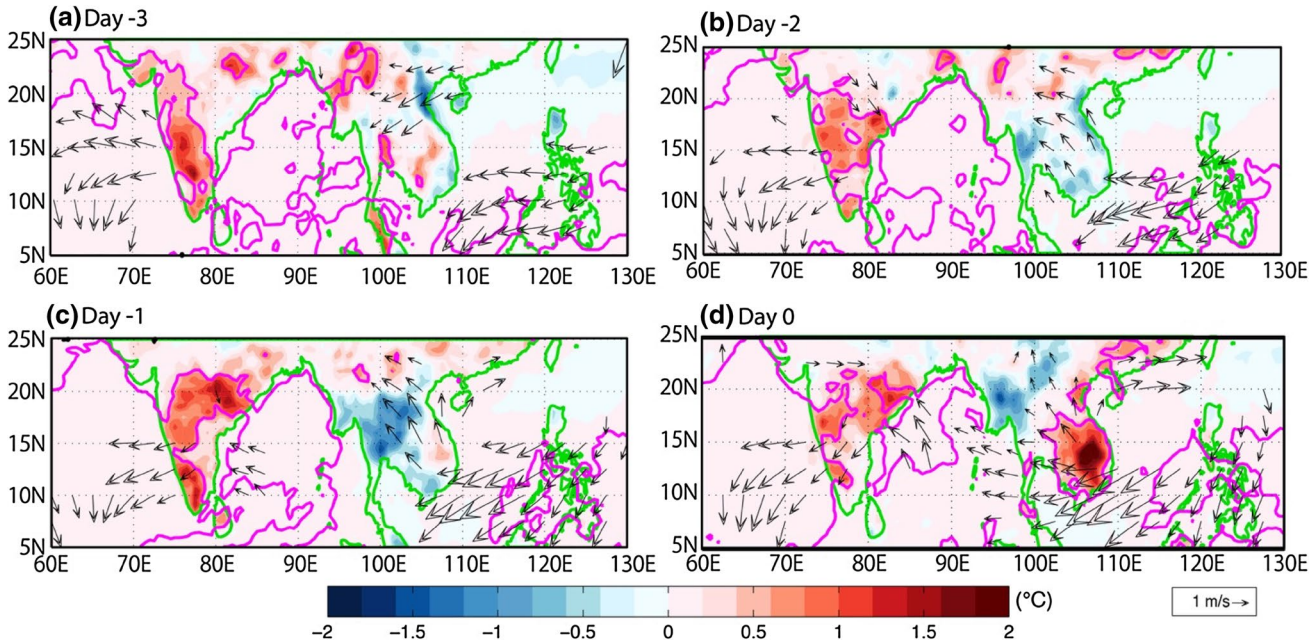

Fig. 5 As in Fig. 4, but for the wet season

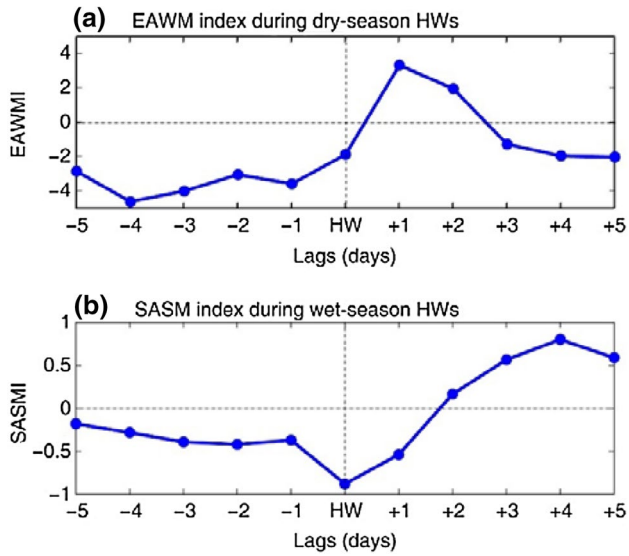

Fig. 6 Composite anomalies of daily EAWM index during HWs in the dry season (top) and daily SASM index during HWs in the wet season (bottom). 'HW' denotes the composite mean over the duration of HWs. Negative (positive) lags denote the composite mean over the period before (after) the HW onset (end), e.g., day −1 (+1) denotes the day before (after) the HW onset (end), and so forth

anomalies of daily EAWM index as defined by (Jhun and Lee 2004) during the HWs in the dry season. As shown in Fig. 6a, the EAWM index exhibit negative anomalies before the Indochina HWs occur (i.e., from day −5 to day −1), suggesting that the EAWM circulation is weakened prior to the Indochina HWs. The EAWM circulation then begins to be reestablished during the HWs and becomes stronger one day after the HW ends.

Compared with the dry season, HWs in the wet season exhibit different development patterns. Three days before the onset of HWs in the wet season (day −3), the positive temperature anomalies mainly appear in the western parts of the Indian subcontinent (Fig. 5a). The high temperatures in India become stronger and wider on the days before the HWs in Indochina begin (day −2 to day −1. Fig. 5b–c), and they are discernible over the Indochina Peninsula on the onset date of Indochina HWs (day 0; Fig. 5d), with a prominent warming center in central Indochina Peninsula.

The development of temperature anomalies in the wet season is associated with the intensification of anomalous easterly wind in the tropics (i.e., along the 10°N–20°N region), which indicates a weakening of the SASM circulation. On day −3, easterly anomalies appear in the eastern Arabian Sea and southern SCS regions. The easterly anomaly in the Arabian Sea extends eastward and reaches the western parts of BOB on day −1. When HWs in Indochina occur (day 0), the easterly anomaly covers the most parts of northern BOB and the Indochina Peninsula. These results suggest that the development of HWs in the wet season is associated with the expansion of the high-temperature anomaly in South Asia and that SASM may play an important role in the occurrence of HWs during the wet season.

Similarly, the composite anomalies of daily SASM intensity as defined by (Webster and Yang 1992) associated with HWs in the wet season are examined (Fig. 6b). The SASM circulation is weakened prior to the

occurrence of HWs in the wet season (i.e., from day −5 to day −1). Particularly, the SASM circulation reaches its weakest state when HWs occur. About two days after the termination of the HWs, the SASM circulation tends to become stronger than normal. These results indicate an important role of the SASM circulation in the HW occurrence in Indochina.

4 Synoptic features and atmospheric controls of heat waves

The above analyses indicate that the high temperature anomalies in the dry and wet seasons start from the northern East Asia and western South Asia, respectively, and they are likely accompanied by the weakening of EAWM and SASM circulations, respectively. To further understand the mechanism for HWs, we examine their typical synoptic behavior and associated large-scale atmospheric circulations in this section. These patterns are detected by examining the composite anomalies of the pertinent variables for the HW events.

4.1 Near-surface patterns

Figure 7 shows the spatial distributions of surface anomalous patterns averaged over the duration of the HWs for the dry season. The fields shown include T_{max}, precipitation amount, SLP, and 850-mb relative humidity. When HWs occur in the dry season, high-temperature anomalies extend beyond the Indochina region and affect southwestern China (Fig. 7a). The Indochina Peninsula region experiences suppressed precipitation (Fig. 7b) and reduced humidity (Fig. 7d). Meanwhile, the decrease in precipitation and humidity can be observed in the SCS and eastern BOB regions. We also notice that this warm and dry anomaly extends upward to the middle atmosphere (not shown). HWs are accompanied by lower than normal SLP over East Asia (Fig. 7c). The low pressure over East Asia is accompanied by an anomalous cyclonic circulation near the surface, with an anomalous southwesterly flow in the eastern part of East Asia (Fig. 10a), implying a weakening of the EAWM circulation. The hot and dry conditions over the Indochina Peninsula may be partially attributed to this weakening of the wintertime monsoon flow.

In the wet season (Fig. 8), HWs in Indochina are accompanied by weak warming anomalies in not only parts of East

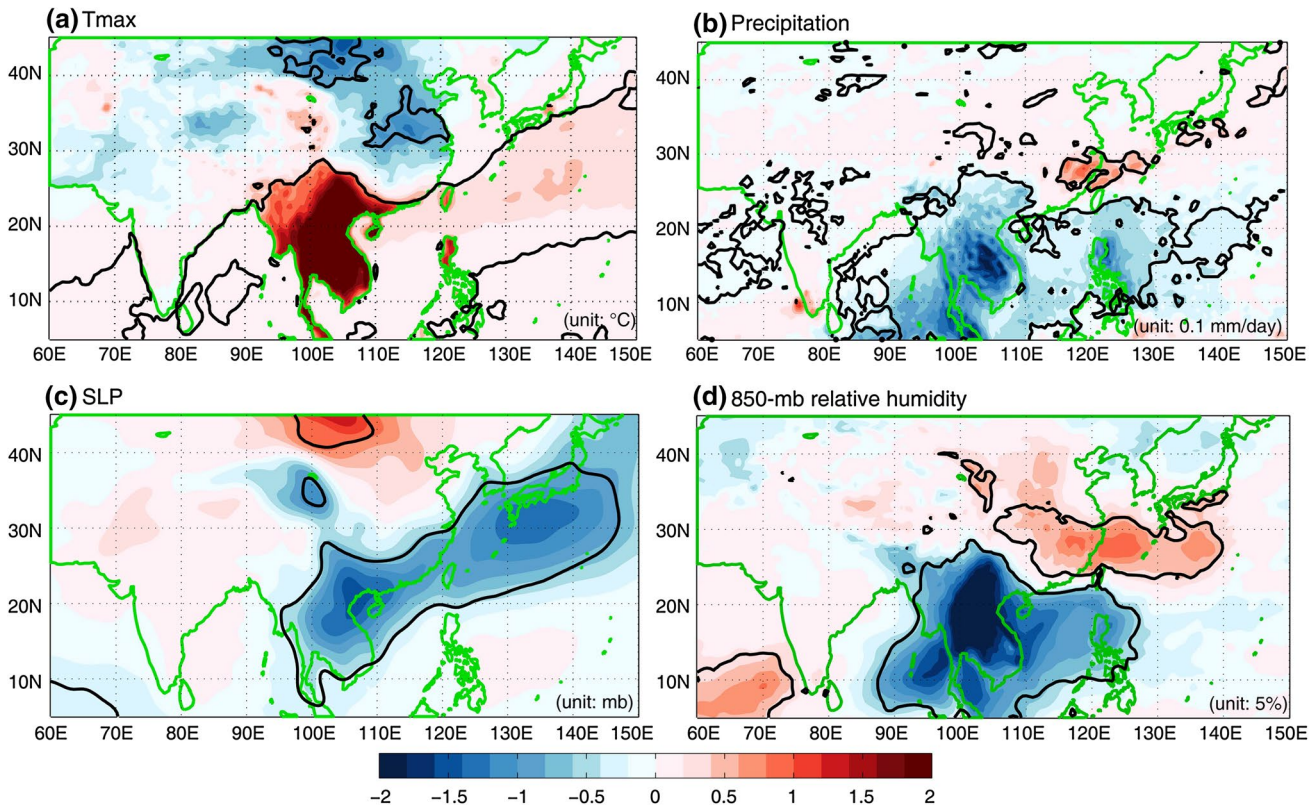

Fig. 7 Composite charts of anomalies of **a** T_{max}, **b** precipitation amount, **c** SLP, and **d** 850-mb relative humidity for HWs in the dry season. Black thick contour denotes significance at the 95% confidence level

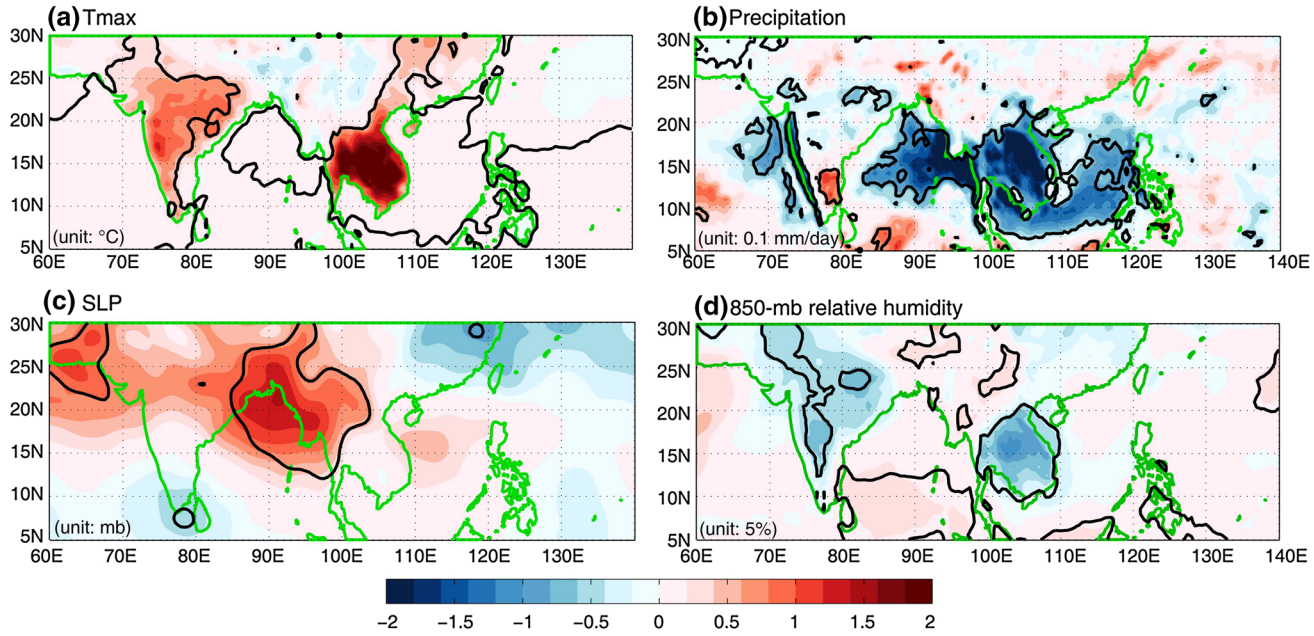

Fig. 8 As in Fig. 7, but for the wet season

Asia but also South Asia such as central and northern India (Fig. 8a). When HWs occur, the precipitation is suppressed and the humidity is decreased over Indochina (Fig. 8b, d). Precipitation decreases also extend to the SCS. Moreover, the precipitation on the western and southwestern sides of the Indochina Peninsula (such as eastern BOB) and the India subcontinent, is noticeably reduced. At the same time, the humidity over the India subcontinent is significantly reduced during HWs in Indochina. HWs in the wet season are accompanied by anomalous high pressure over the northeastern BOB and northern SCS (Fig. 8c). These SLP features are coincident with anomalous low-level anticyclonic circulations (Fig. 10b). These anticyclones are associated with anomalous easterly wind along the tropical region (i.e., the 10°N–20°N zone), and indicate a weakening of the SASM westerly flow.

4.2 Vertical structures

Figure 9 shows the longitude-height sections of geopotential height and pressure velocity along the zone between 10°N and 20°N. In the case of dry seasons (Fig. 9a), negative height anomalies are found at the low-level, corresponding to the decreased sea level pressure there (see Fig. 7a). However, at the middle- and upper-levels, Indochina and nearby regions are covered by significantly increased geopotential height. These patterns suggest that HWs in the dry season are associated with a warm-core low structure. More importantly, anomalous sinking air column covers the whole Indochina region (as shown in shadings of Fig. 9a), extending eastward to the regions of the SCS and the Philippine Sea. Such sinking anomalies suggest weakened convective activity, thus leading to suppressed precipitation over these areas (see Fig. 7b).

In the wet season (Fig. 9b), the Indochina and SCS regions (i.e., 90°E–120°E) are covered by positive height anomalies, with the most significant anomaly appearing in the middle atmosphere, showing that HWs in the wet season is characterized by a warm-core high structure. On the other hand, negative anomalies are observed on the east side of these regions, indicating a westward extension of WNPSH. This finding suggests that WNPSH may play an important role in the Indochina HW. Figure 9b also shows that HWs in the wet season of the Indochina are coincident with an anomalously sinking air column above that region. This downward anomaly weakens the convection and decreases precipitation, thus contributing to HWs in this region.

4.3 Large-scale circulation patterns

The roles of EAWM and SASM in the development of HWs in dry and wet seasons are further detected by examining the large-scale circulation patterns shown in Fig. 10. The composite anomalies of 850-mb horizontal wind and velocity potential for HWs in the dry season are displayed in Fig. 10a. This chart indicates that HWs are associated with a cyclonic anomaly over eastern China, with anomalous southwesterly flow over the most parts of East Asia. These wind anomalies imply a weakening of the northeasterly flow of the EAWM circulation and reinforce the notion of a significant role of

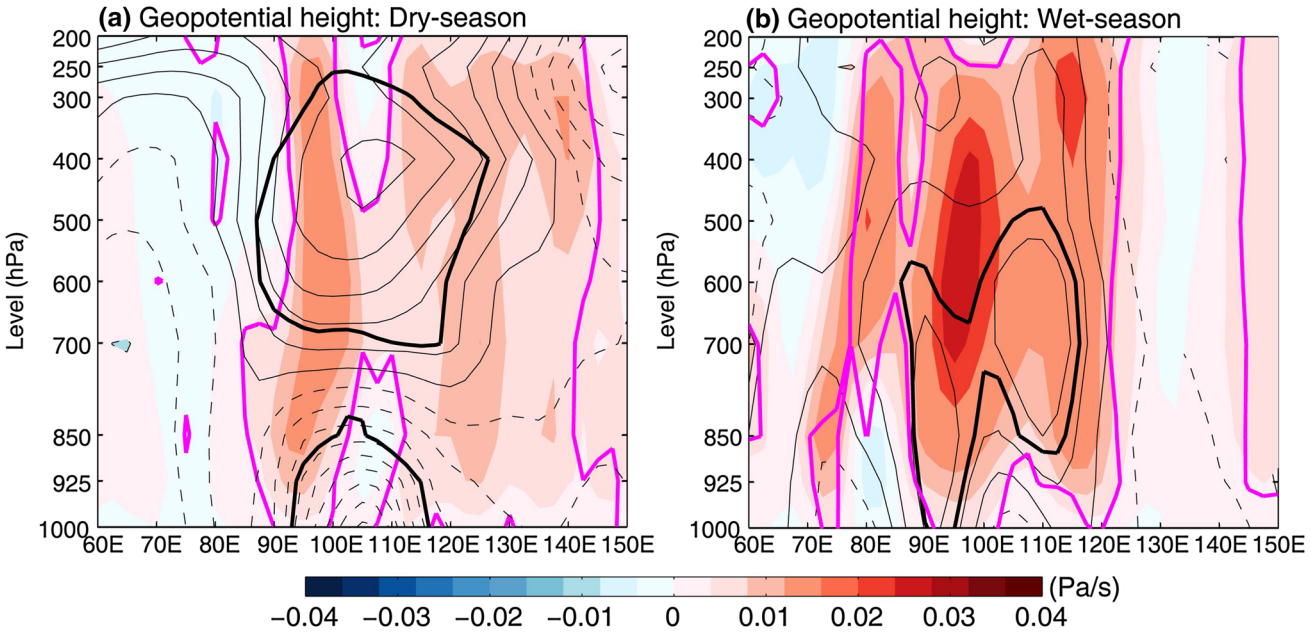

Fig. 9 Composite anomalies of pressure velocity (shading) and geopotential height (contour) and for HWs in the dry (left) and wet (right) seasons. Longitude-height cross section is averaged over the latitudes between 10°N and 20°N. Solid and dashed contour denote positive and negative geopotential height anomalies, respectively. Black and purple thick curves respectively indicate the significant anomalies of geopotential height and pressure velocity at the 95% confidence level

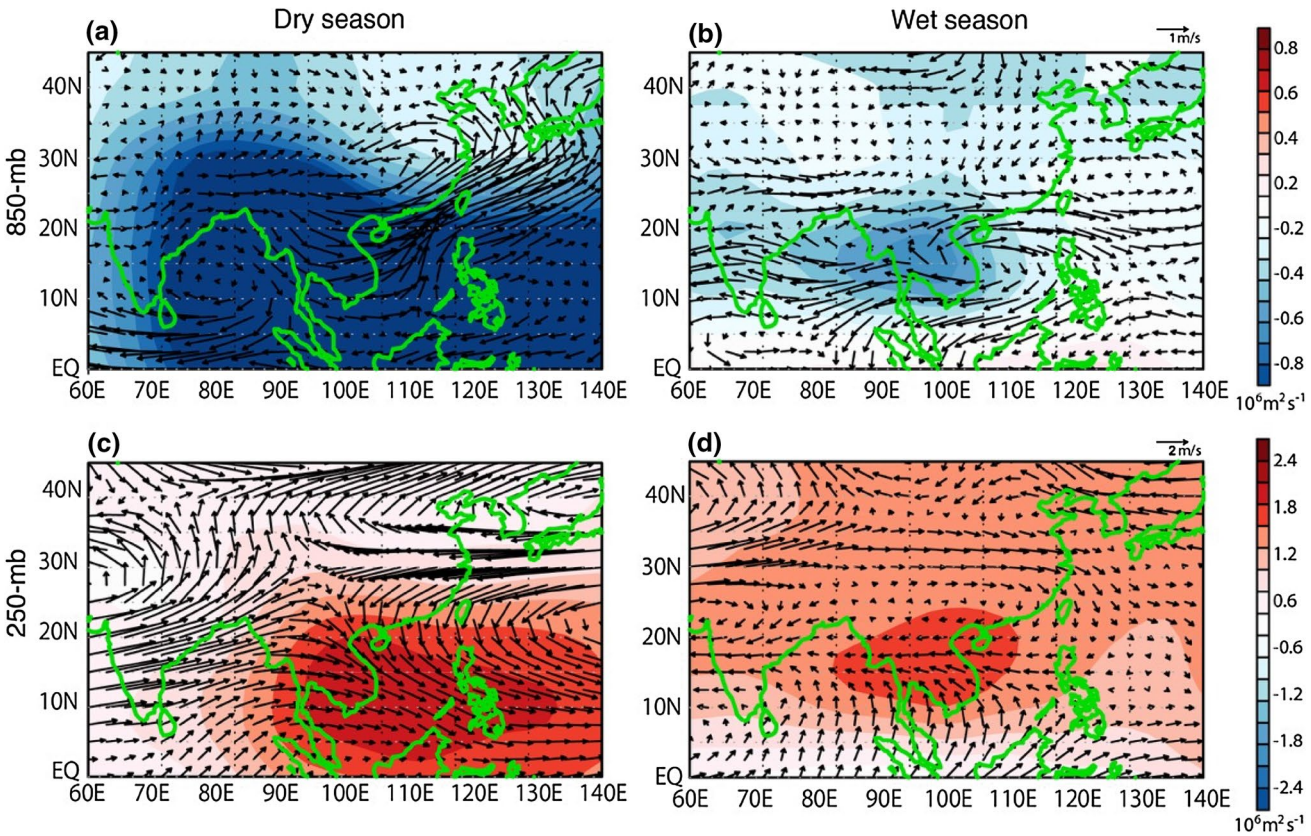

Fig. 10 Composite charts of anomalies of horizontal winds (vectors) and velocity potential (shading) at (top) 850-mb and (bottom) 250-mb levels for HWs in the dry (left) and wet (right) seasons

the EAWM in HW occurrences in the Indochina Peninsula during the dry season. On the other hand, Fig. 10b shows the low-level wind pattern for HWs in the wet season. This pattern is characterized by strongly anomalous easterly wind in the tropical regions such as southern parts of SCS, Indochina, and BOB, and most parts of the Indian subcontinent. These easterly anomalies are situated to the south of two anomalous anticyclones over the northern BOB and central SCS, respectively.

In the upper troposphere, the most prominent feature associated with HW events in Indochina in the dry season (Fig. 10c) is the anomalous easterly flow over eastern China and southern Japan, which is located to the south of an anomalous anticyclone centered over northern China and Korea. This feature indicates that the prevalent subtropical westerly jet stream in that region is weaker than normal during the HW events. In this environment of weaker jet stream intensity and hence weakened baroclinic disturbances, it is anticipated that the winter monsoon activity over East Asia would also decrease. In the wet season, HWs in Indochina are coincident with an anomalous 250-mb cyclonic pattern to the northwest of the Tibetan Plateau (Fig. 10d). This feature suggests that the prevalent upper tropospheric high pressure center over that region (often referred as the 'Tibetan Anticyclone') would be weaker than normal during HW events in Indochina. Since the strength of the Tibetan Anticyclone is closely related to the intensity of the SASM (e.g., see Zhang et al. (2002)), the result in Fig. 10d is consistent with our earlier claim that HW events in Indochina during the wet season typically occur when the SASM circulation is weak.

Figure 10 also portrays anomalous velocity potential in lower and upper atmosphere associated with HWs in Indochina. For HWs in the dry season (the left column of Fig. 10), a prominent divergent center is evident at the lower atmosphere over Indochina (blue shadings in Fig. 10a) and a convergent center appears in the upper atmosphere (red shadings in Fig. 10c). These two centers indicate anomalous subsidence over the Indochina Peninsula. This sinking air motion contributes to the warm and dry conditions in that region.

The above patterns for the dry season are similar to the corresponding charts for the wet season (the right column of Fig. 10). HWs in the wet season are accompanied by a divergent center at the lower level (Fig. 10b) and a convergent center at the upper level (Fig. 10d), thus also implying anomalous downward circulation.

4.4 HWs in strong and weak monsoon years

The above results show that the intra-seasonal weakening of EAWM and SASM circulations could contribute to HW occurrences in the dry and wet season of Indochina,

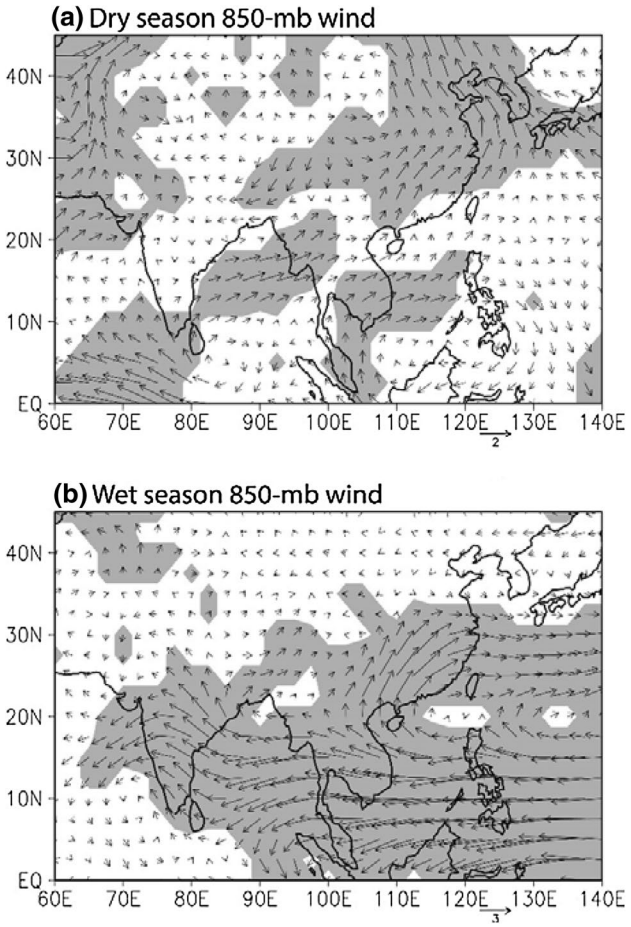

Fig. 11 Differences of 850-mb wind in the (top) dry and (bottom) seasons between strong and weak monsoon years (i.e., weak minus strong years). Shading denotes significance either for zonal or meridional components at the 95% confidence interval

respectively. In this subsection, the HW measures during strong and weak monsoon years are compared at annual scale. We first remove the long-term trends of HW metrics and then obtain the difference in the detrended HW metrics between weak and strong monsoon years (i.e., weak years minus strong years). A weak (strong) monsoon year is defined when the monsoon index is smaller (larger) than its mean value by one standard deviation.

As listed in Table 1, compared with strong EAMW/SASM years, all HW measures in the weak EAMW/SASM years are intensified. On average, the seasonal mean T_{max} in weak EAMW (SASM) years is 1.11 (0.55) °C higher than strong EAMW (SASM) years. Weak EAMW (SASM) is associated with more 0.2 (1.54) HW events and 9.64 (24.22) HW days than strong EAMW (SASM). HWA and HWM in weak EAMW (SASM) years are 0.18 (0.37) and 0.07 (0.01) °C higher than strong years. In addition, compared with strong EAMW (SASM) years, HWs in weak EAMW (SASM) years tend to occur and end later.

Possible influences of monsoon circulations on HWs in Indochina can be observed by probing into the composite difference of 850mb horizontal wind between weak and strong monsoon years. In the dry season (Fig. 11a), an anomalous cyclone prevails over mainland China, with anomalous southwesterly flow over most parts of East Asia. This weakening of the northeasterly flow of the EAWM circulation is in accord with the results in Fig. 10a, indicating that a weakening EAWM circulation favors the HWs in Indochina. During weak SASM years (Fig. 11b), strong anomalous easterly wind appears in the tropical regions. These easterly anomalies are situated to the south of two anomalous anticyclones over the northern BOB and central SCS. Again, these patterns are close to those in Fig. 10b, suggesting a weakened SASM circulation can provide a favorable environment for intensifying the wet-season HWs.

5 Long-term changes of heat waves

Figure 12 depicts the occurrence of the identified HWs in various years. It shows that for both dry and wet seasons, HW events are becoming more frequent in the latter part of the study period. HWs in both seasons are ending later and commencing slightly earlier. HWs in dry season mainly occurred in the middle to late March and April in the 1980s and early 1990s, while they became more frequent in early March (even as early as late February) and early May in more recent years. Compared with the dry season, the progressively broader spread of HW occurrences across various calendar months is more evident in the wet season.

More specifically, Figs. 13 and 14 show the time series of various aspects of HW activities as computed for HWs in the dry and wet seasons, respectively. Their estimated long-term trends are listed in Table 2. It is shown in Fig. 13 that all measures for HWs in the dry season except for HWL and HWO exhibit prominent upward trends. The T_{max} averaged throughout the dry season shows a warming trend of 0.15 °C per decade (Fig. 13a). HWN has been increasing significantly by 0.45 events per decade since 1979 (Fig. 13b). HWF bears a trend of + 3.75 days per decade (Fig. 13c). HWD exhibits a slight prolonging trend of 0.34 days per decade (Fig. 13d), suggesting that the longest HW of the year is becoming longer. However, HWL has a slight shortening trend (Fig. 13f). Regarding the HW severity, HWA shows a significant intensifying trend of 0.34 °C per decade (Fig. 13e), implying that the HW amplitude is becoming stronger. Compared with HWA, HWM has a relatively weaker increasing trend (Fig. 13g), i.e., 0.07 °C per decade.

Besides the duration and severity of HWs, we also examine the trends of the timing of HWs during the 1979–2010 period. Figure 13h depicts the time series of HWO (i.e., the onset date of the first HW event) and HWE (i.e., the ending date of the last event) in the dry season. The onset date (i.e., HWO) exhibits a downward trend of 3.57 days per decade, suggesting that the HWs in the dry season are commencing earlier. Moreover, the ending date (i.e., HWE) exhibits a prominent upward trend of 12.31 days per decade, indicating that the HWs in the dry season are terminating later in the calendar year.

The trends in HW measures in the wet season are even stronger (mostly by a factor of 2–3) than those in the dry season. Figure 14 shows the time series of the HW measures

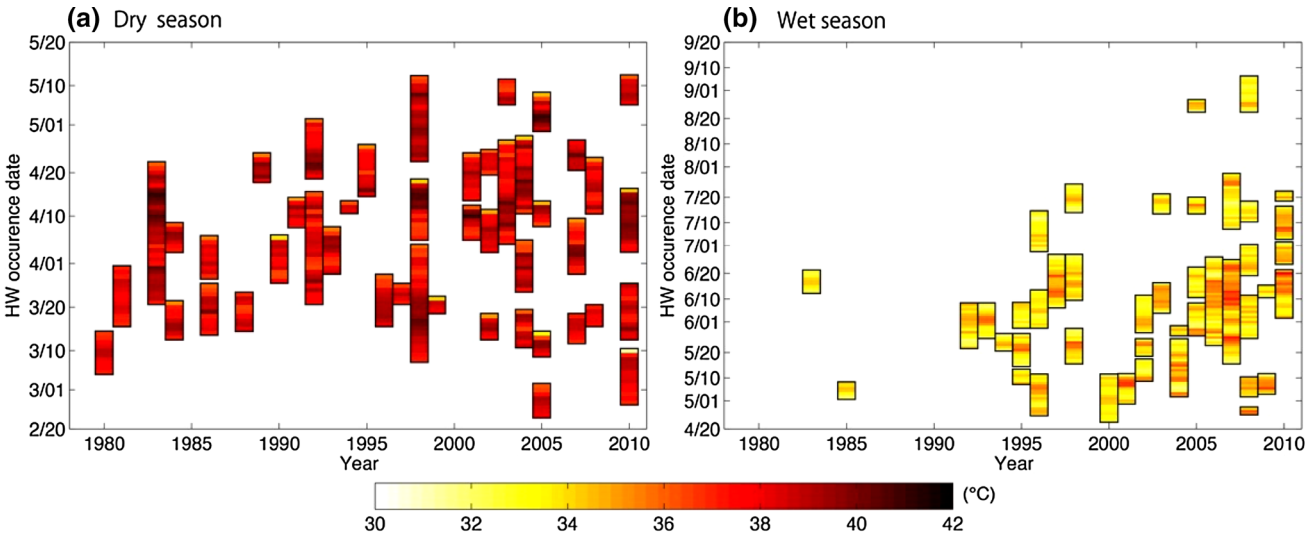

Fig. 12 Occurrences of regional HWs in the Indochina Peninsula in the dry (left) and wet (right) seasons of 1979–2010. Shading indicates the spatial average of T_{max} during HWs

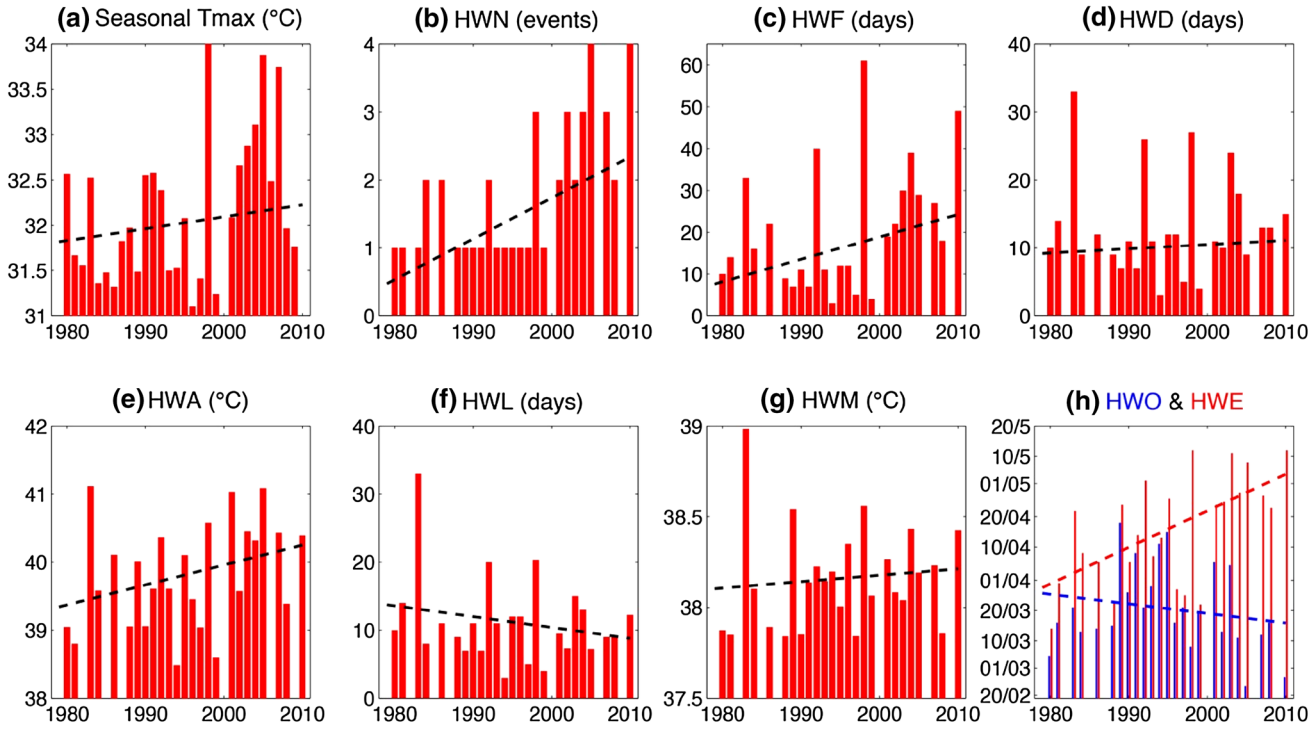

Fig. 13 Time series of **a** seasonal mean T_{max}, **b** HWN, **c** HWF, **d** HWD, **e** HWA, **f** HWL, **g** HWM, **h** HWO (blue strips) and HWE (pink strips) for HWs in the dry season. Straight lines indicate their corresponding linear trends

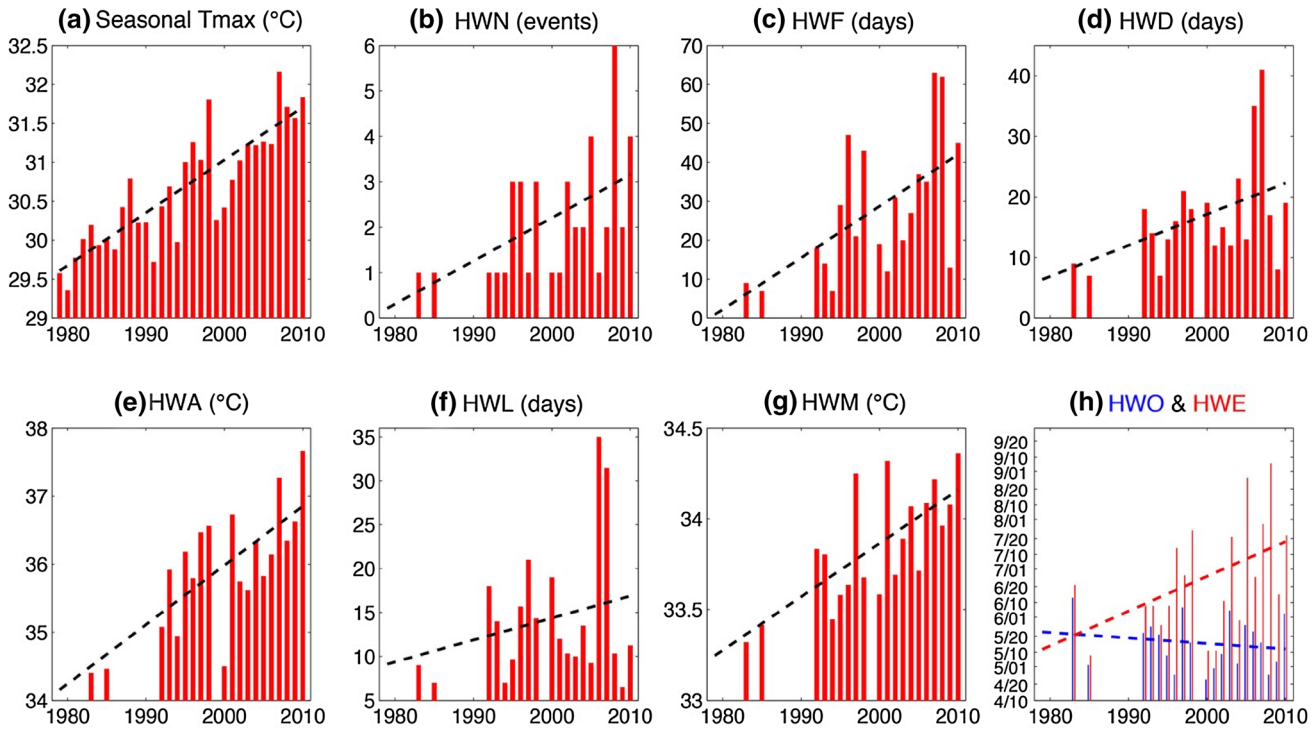

Fig. 14 As in Fig. 13, but for the wet season

Table 2 HW trends (per decade) in the dry and wet seasons of 1979–2010 in the Indochina Peninsula

HW measures	Trend in dry season	Trend in wet season
Seasonal T_{max}	+ 0.15	+ **0.67**
HWN	+ **0.45**	+ **0.87**
HWF	+ **3.75**	+ **14.0**
HWD	+ 0.34	+ **7.22**
HWA	+ **0.34**	+ **1.05**
HWL	− 0.76	+ 0.48
HWM	+ **0.07**	+ **0.37**
HWO	− 3.57	− 4.0
HWE	+ **12.31**	+ **23.89**

Bold values denote significance at the 95% confidence level, as obtained by a modified Mann–Kendall trend test (Hamed and Rao 1998)

as computed for HWs in the wet season and their long-term trends are given in Table 2. The T_{max} averaged throughout the wet season bears a significant warming trend of 0.67 °C per decade (Fig. 14a). HWN and HWF exhibit increasing trends of 0.87 events and 14.0 days per decade, respectively (Fig. 14b,c). Meanwhile, there are also prolonging trends in the duration of HWs in the wet season. For instance, HWD exhibits a prolonging trend of 7.22 days per decade (Fig. 14d), and HWL (i.e., the average length of all yearly events) has an upward trend of 0.48 days per decade (Fig. 14f). Regarding the severity of HWs in the wet season, HWA and HWM show increasing trends of 1.05 and 0.37 °C per decade, respectively (Fig. 14e,g). Figure 14h depicts the time series of HWO and HWE of HWs in the wet season. It indicates that the onset date HWO exhibits an advancing trend of 4.0 days per decade while HWE exhibits a delaying trend of 23.89 days per decade.

Figure 15 depicts the evolution of the distribution of T_{max} in the dry and wet seasons from 1979 to 2010. It shows that T_{max} in the dry and wet seasons exhibit bimodal and unimodal distributions, respectively. The two peaks (at ≈30 °C and ≈36 °C, respectively) in the bimodal distribution of the dry season correspond to the two subperiods that exhibit remarkably different temperatures, i.e., a relatively cool subperiod from November to January and a hot subperiod from February to May (see Fig. 2a). Figure 15 shows that the overall distribution of T_{max} is shifted towards higher values in 1979–2010, i.e., +0.15 and 0.67 °C per decade for dry and wet seasons, respectively. However, the skewness of the distribution does not exhibit significant long-term changes (p-value > 0.05). These findings demonstrate that the intensifying trend in HW activities is mainly due to the shift of the T_{max} distribution, rather than its shape. During the 1979–2010 period, the global temperature (over land and ocean) has also been increasing by 0.14–0.18 °C per decade (Grant and Stefan 2011). This global trend is slower than the trend of temperature in Indochina, implies that the warming temperature and intensifying HWs in Indochina could also be affected by other factors, e.g., the possible changes in the associated atmospheric circulations (as discussed in the following sections).

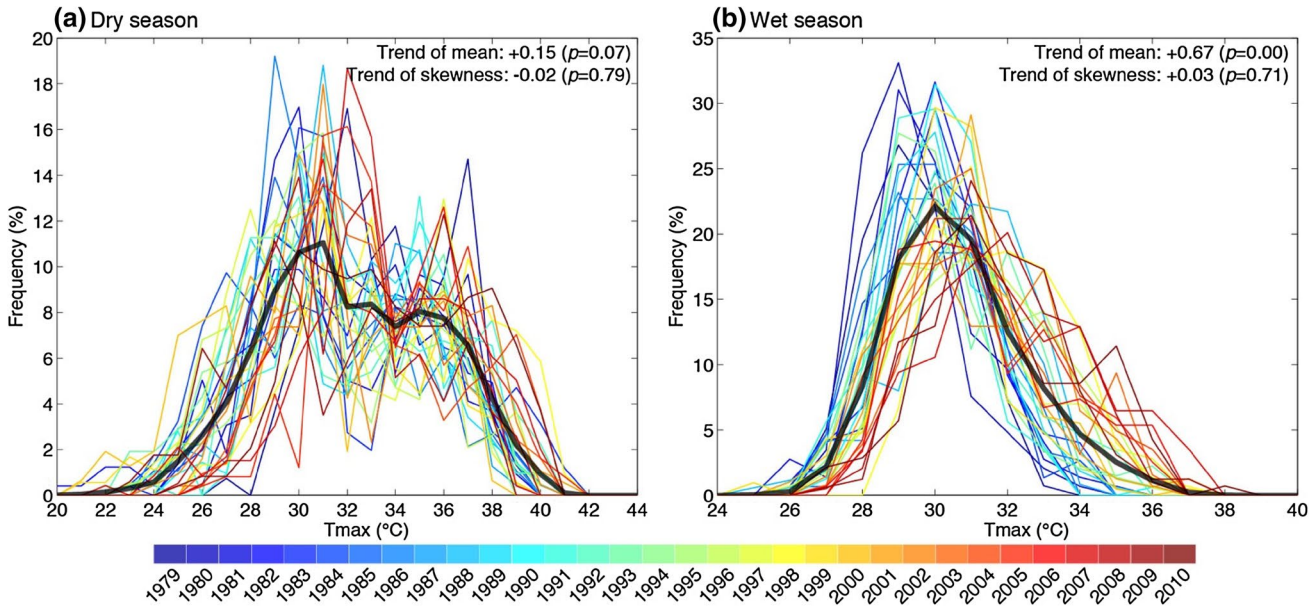

Fig. 15 Frequency distribution of T_{max} in the dry (left) and wet (right) season for individual years within the 1979–2010 period. Results for various years are indicated using different colors as depicted by the bar at the bottom. Thick curve denotes the average of T_{max} distribution. Numbers in the upper right corner of each panel indicate the long-term trends of T_{max} mean (in °C per decade) and skewness (per decade), and the numbers in bracket are their p-values as obtained from the significance test

6 Conclusion

A remarkable displacement exists in the seasonal cycles of temperature and precipitation in the Indochina Peninsula. The highest temperature occurs in the dry early spring season, while relatively lower temperature prevails in the summer wet season. In this study, we examine and compare the characteristics of HWs occurring in the dry and wet seasons of the Indochina Peninsula.

HWs in both seasons are accompanied by negative anomalous precipitation, and the Indochina region is covered by a dry and hot atmospheric column. When HWs occur, the Indochina and nearby regions are covered by anomalous downward air movement, which contributes to the dry conditions over the region. HWs in dry and wet seasons are associated with rather distinct large-scale atmospheric settings, i.e., weakening of the EAWM and SASM circulations, respectively. On the one hand, HWs in the dry season are accompanied by an anomalous cyclone over eastern China and southwesterly flow over East Asia, which are signatures of a weakened EAWM circulation. Moreover, HWs in Indochina are also coincident with high-temperature anomalies over East Asia. On the other hand, HWs in the wet season are characterized by anomalous easterlies lying to the south of anticyclones over BOB and SCS, which are indicative of a diminished SASM in that region. This relationship is further substantiated by the prevalence of warm temperature anomalies over South Asia (i.e., Indian subcontinent) during HW episodes in the wet season of the Indochina Peninsula (Fig. 5).

We also find that HW metrics for both dry and wet seasons exhibit prominent upward trends during 1979–2010, in terms of frequency and amplitude. Particularly most upward trends of HWs in the wet season are about two to three times stronger than those in the dry season. We also notice that the onset (termination) of HWs in the two seasons have occurred progressively earlier (later) in the seasonal calendar in recent decades.

7 Discussions

In this study, we have chosen our study domain to be the Indochina region with climatological mean T_{max} higher than 30 °C. To examine the dependence of our findings on this particular choice, we have compared the HW behavior in different subregions of the Indochina Peninsula (not shown). Eight subregions are identified by applying a rotated empirical orthogonal function (REOF) analysis on the T_{max} anomalies. HWs are then defined on the basis of each of these eight REOF subregions, and their characteristics are examined accordingly. We find that HW metrics in all subregions are characterized by prominent upward trends in both dry and wet seasons. The synoptic behavior and large-scale atmospheric environments of HWs in these subregions are very similar to those derived from our study region (i.e., central Indochina), with some slight differences in amplitude and geographical location. Therefore, the characteristics of HWs in central Indochina are applicable to other subregions of Indochina.

The primary dataset used in the current study is the CFSR reanalyses. Previous studies have demonstrated its utility for studying various regional details of the observed atmospheric circulation (Lau and Nath 2012, 2014; Luo and Lau 2017). Nevertheless, it is also worthwhile to study the HW behavior in the Indochina Peninsula by using model simulations. A vigorous comparison between the results based on observations and model output, and a more incisive diagnosis of the model-simulated HW events, may unravel the myriad processes and mechanisms contributing to the onset, maintenance, and termination of HWs in Indochina.

In our study, HWs in the dry and wet seasons of Indochina are considered separately. These seasons are determined by the monsoon onset and withdrawal dates. Monsoon onset in mid-May has been defined by many different variables such as precipitation (Htway and Matsumoto 2011; Wang and LinHo 2002; Zhang et al. 2002), saturated equivalent potential temperature (Zhang et al. 2004), and low-level wind (Lin and Luo 2017; Wang et al. 2004). Here we adopt the definition by Zhang et al. (2002) by using 5 mm/day precipitation as the threshold. We have extended this definition to the monsoon withdrawal phase by noting the timing of the abrupt precipitation decrease to below the 5 mm/day level in mid-October (Fig. 2b). Alternative thresholds, e.g., 4 mm/day, have been used in other studies (Abe et al. 2013; Chen 2006). However, using the 4 mm/day threshold yields nearly the same set of HW occurrences as our present results. The agreement among identified HW episodes based on different precipitation thresholds is due to the fact that the HWs mainly occur in the middle of the season (either dry or wet seasons), and seldom appear during the transition phase of monsoon circulation (e.g., see Fig. 12).

Besides the classification according to the dry/wet seasons, HWs could also be defined by either daily T_{max} or T_{min} series using absolute or relative thresholds (Perkins 2015; Perkins and Alexander 2013; You et al. 2017). Due to the difference in the magnitude of temperature in the dry and wet seasons of Indochina (see Sect. 2.2), relative thresholds are more appropriate for this comparative analysis among dry and wet seasons. Besides, we select T_{max} because it is in accordance with common climatological practice in many regions such as Czech Republic (Huth et al. 2000), Denmark (Christensen 2006), Sweden (Åström et al. 2014), Netherlands (Huynen et al. 2001), and China (Xu et al. 2009).

T_{max}-derived HWs have also been shown to be closely associated with substantial societal impacts on human health and economies (Beniston 2004; Meehl and Tebaldi 2004).

Previous works suggest that the westward extension of WNPSH plays an important role in HWs or extreme high tempertures in East Asia (Luo and Lau 2017; Wang et al. 2014). Here we also examine the composite charts of anomalies of 500-mb geopotential height prior to the occurrence of HWs in Indochina (Fig. 16). This result indicates that the westward extension of WNPSH corresponds well to the initiation of HWs in the wet season. Three days before the beginning of a typical HW (day −3), an extension of WNPSH appears over the Philippine Sea. This extension continues to strengthen and moves westward into southern China (day −2). On the day before the HW starts (day −1), the extended WNPSH dominates most parts of southern China and reaches the eastern Indochina. On the day when the HW begins (day 0), the extended WNPSH covers most parts of the Indochina Peninsula. Compared with HWs in the wet season, possible role of WNPSH in HWs in the dry season is marginal (not shown).

As suggested by previous studies, WPNSH plays an important role in extreme high temperatures or HWs in many Asian regions such as South and Southeast China (Ding et al. 2010; Luo and Lau 2017; Wang et al. 2013, 2014, 2016). Similar to HWs in Indochina, HWs in these regions are also often accompnaied by suppressed preciptation, anomalously dry and sinking air column, and higher presure and anticyclonic anomalies at low-level. Wang et al. (2016) have examined three typical HWs in the summers of 2003, 2006, and 2013 in southeasten, southwestern, and eastern China, respectively. They found that the HWs in 2003 and 2013 were associated with a southward displacement of EAJS and weatward intensificaiton of WNPSH; while the HW in 2006 was characterzied by negative SLP and geopotential height anomalies, and poleward displacement of EAJS. In our study, we have also noticed that HWs in the dry season is accompanied by a weakened prevalent subtropical westerly jet stream (Fig. 10c).

In this study, we found that various aspects of HW in Indochina show significant trends of intensification. These trends are not only attributable directly to global warming, but may also be related to long-term changes in the ambient atmospheric circulation. As shown in Sect. 4, the weakening of the EAWM and SASM circulations provides favorable conditions for HWs in the dry and wet seasons, respectively. Moreover, both EAWM and SASM weakened significantly after the 1980s (Fan et al. 2010; Wang and Chen 2010; Wang et al. 2009). These weakening trends in monsoon circulation are in accord with the intensifying trends of HW activities

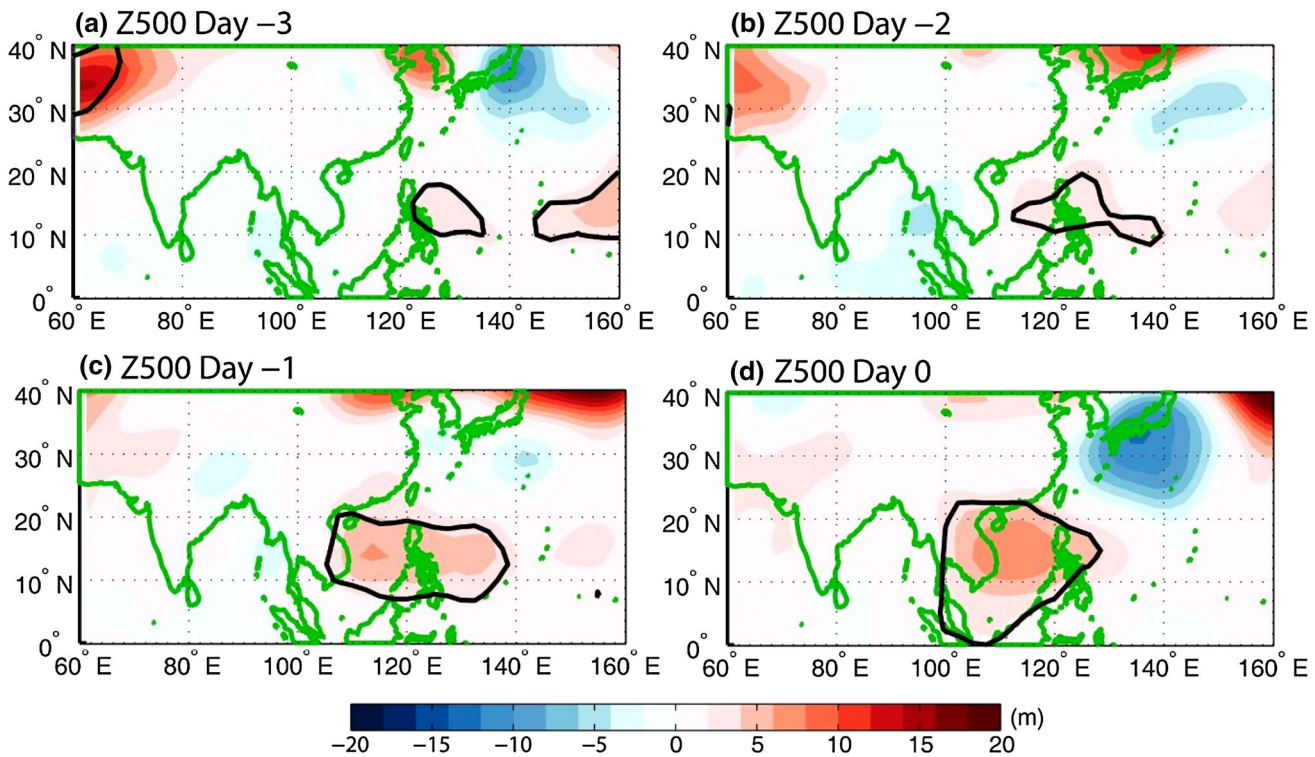

Fig. 16 Composite charts of anomalies of 500-mb geopotential height prior to the occurrence of HW in the wet season. Day 0 denotes the onset day of the HW event. Day −1 denotes the day before Day 0, and so forth. Thick contour denotes significant positive anomalies at the 95% confidence level

during 1979–2010. This correspondence implies that the intensifying HW activities may be due to the weakening EAWM and SASM circulations to some degree. Following this line of reasoning, we anticipate that HW activities in both seasons will become more frequent and stronger in the coming decades, since both the strength of EAWM and SASM circulations is projected to decrease in the future (Hong et al. 2017; IPCC 2013).

Acknowledgements This study is partially supported by the National Natural Science Foundation of China (no. 41401052). The appointment of NCL at The Chinese University of Hong Kong is partially supported by the AXA Research Fund. The appointment of ML at The Chinese University of Hong Kong is supported by the Postdoctoral Fellowship Scheme of the Faculty of Social Science (no. 3132220) and the Focused Innovations Scheme (no. 1907001).

References

Abe M, Hori M, Yasunari T, Kitoh A (2013) Effects of the Tibetan Plateau on the onsetof the summer monsoon in South Asia: the role of the air-sea interaction. J Geophys Res Atmos 118:1760–1776

Anderson GB, Bell ML (2011) Heat waves in the United States: mortality risk during heat waves and effect modification by heat wave characteristics in 43 US communities. Environ Health Perspect 119:210–218

Åström C, Ebi KL, Langner J, Forsberg B (2014) Developing a heatwave early warning system for Sweden: evaluating sensitivity of different epidemiological modelling approaches to forecast temperatures. Int J Environ Res Public Health 12:254–267

Beniston M (2004) The 2003 heat wave in Europe: a shape of things to come? An analysis based on Swiss climatological data and model simulations. Geophys Res Lett 31:L02202

Brunner L, Hegerl GC, Steiner AK (2017) Connecting atmospheric blocking to European temperature extremes in spring. J Clim 30:585–594

Chang C-P (2004) East Asian monsoon, vol 2. World Scientific, Singapore

Chen T-C (2006) Variation of the Asian monsoon water vapor budget: interaction with the global-scale modes. In: Wang B (ed) Asian Monsoon. Springer, Berlin, p 417–457

Christensen OB (2006) Regional climate change in Denmark according to a global 2-degree-warming scenario. Danish Climate Centre Report 06–02. Danish Meteorological Institute, Ministry of Transport and Energy, p 17

Christidis N, Stott PA, Brown SJ (2011) The role of human activity in the recent warming of extremely warm daytime temperatures. J Clim 24:1922–1930

Christidis N, Jones GS, Stott PA (2015) Dramatically increasing chance of extremely hot summers since the 2003 European heatwave. Nature Climate Change 5:46–50

Coumou D, Rahmstorf S (2012) A decade of weather extremes. Nat Clim Change 2:491–496

Ding T, Qian W, Yan Z (2010) Changes in hot days and heat waves in China during 1961–2007. Int J Climatol 30:1452–1462

Dole R, Hoerling M, Perlwitz J, Eischeid J, Pegion P, Zhang T, Quan XW, Xu T, Murray D (2011) Was there a basis for anticipating the 2010 Russian heat wave? Geophys Res Lett 38:L06702

Fan F, Mann ME, Lee S, Evans JL (2010) Observed and modeled changes in the South Asian summer monsoon over the historical period. J Clim 23:5193–5205

García-Herrera R, Díaz J, Trigo R, Luterbacher J, Fischer E (2010) A review of the European summer heat wave of 2003. Crit Rev Environ Sci Technol 40:267–306

Grant F, Stefan R (2011) Global temperature evolution 1979–2010. Environ Res Lett 6:044022

Grotjahn R, Black R, Leung R, Wehner MF, Barlow M, Bosilovich M, Gershunov A, Gutowski WJ, Gyakum JR, Katz RW, Lee Y-Y, Lim Y-K (2016) North American extreme temperature events and related large scale meteorological patterns: a review of statistical methods, dynamics, modeling, and trends. Clim Dyn 46:1151–1184

Guirguis K, Gershunov A, Schwartz R, Bennett S (2011) Recent warm and cold daily winter temperature extremes in the Northern Hemisphere. Geophys Res Lett 38:L17701

Hamed KH, Rao AR (1998) A modified Mann Kendall trend test for autocorrelated data. J Hydrol 204:182–196

Hong J-Y, Ahn J-B, Jhun J-G (2017) Winter climate changes over East Asian region under RCP scenarios using East Asian winter monsoon indices. Clim Dyn 48:577–595

Htway O, Matsumoto J (2011) Climatological onset dates of summer monsoon over Myanmar. Int J Climatol 31:382–393

Hu K, Huang G, Huang R (2011) The impact of tropical Indian ocean variability on summer surface air temperature in China. J Clim 24:5365–5377

Hu K, Huang G, Wu R (2013) A strengthened influence of ENSO on August high temperature extremes over the southern Yangtze River valley since the late 1980s. J Clim 26:2205–2221

Huang R, Chen J, Wang L, Lin Z (2012) Characteristics, processes, and causes of the spatio-temporal variabilities of the East Asian monsoon system. Adv Atmos Sci 29:910–942

Huth R, Kyselý J, Pokorná L (2000) A GCM simulation of heat waves, dry spells, and their relationships to circulation. Clim Change 46:29–60

Huynen MM, Martens P, Schram D, Weijenberg MP, Kunst AE (2001) The impact of heat waves and cold spells on mortality rates in the Dutch population. Environ Health Perspect 109:463–470

IPCC (2012) Managing the risks of extreme events and disasters to advance climate change adaptation: special report of the intergovernmental panel on climate change. Cambridge University Press, Cambridge, p 582

IPCC (2013) Climate change 2013: the physical science basis. contribution of working group I to the fifth assessment report of the intergovernmental panel on climate change. Cambridge University Press, Cambridge, p 1535

Jhun JG, Lee EJ (2004) A new East Asian winter monsoon index and associated characteristics of the winter monsoon. J Clim 17:711–726

Kenyon J, Hegerl GC (2008) Influence of modes of climate variability on global temperature extremes. J Clim 21:3872–3889

Lau N-C, Nath MJ (2012) A model study of heat waves over North America: meteorological aspects and projections for the twenty-first century. J Clim 25:4761–4784

Lau N-C, Nath MJ (2014) Model simulation and projection of European heat waves in present-day and future climates. J Clim 27:3713–3730

Lin L, Luo M (2017) Objective determination of the onset and withdrawal of the South China Sea summer monsoon. Atmos Sci Lett 18:276–282

Loikith PC, Broccoli AJ (2012) Characteristics of observed atmospheric circulation patterns associated with temperature extremes over North America. J Clim 25:7266–7281

Luo M, Lau N-C (2017) Heat waves in southern China: Synoptic behavior, long-term change, and urbanization effects. J Clim 30:703–720

Marks D (2011) Climate change and Thailand: impact and response. Contemp Southeast Asia J Int Strateg Aff 33:229–258

Matsueda M (2011) Predictability of Euro-Russian blocking in summer of 2010. Geophys Res Lett 38:L06801

Meehl GA, Tebaldi C (2004) More intense, more frequent, and longer lasting heat waves in the 21st century. science 305:994–997

Miralles DG, Teuling AJ, Van Heerwaarden CC, de Arellano JV-G (2014) Mega-heatwave temperatures due to combined soil desiccation and atmospheric heat accumulation. Nat Geosci 7:345–349

Perkins SE (2015) A review on the scientific understanding of heatwaves—their measurement, driving mechanisms, and changes at the global scale. Atmos Res 164:242–267

Perkins SE, Alexander LV (2013) On the measurement of heat waves. J Clim 26:4500–4517

Pfahl S, Wernli H (2012) Quantifying the relevance of atmospheric blocking for co-located temperature extremes in the Northern Hemisphere on (sub-) daily time scales. Geophys Res Lett 39:L12807

Pfahl S, Schwierz C, Croci-Maspoli M, Grams CM, Wernli H (2015) Importance of latent heat release in ascending air streams for atmospheric blocking. Nat Geosci 8:610–614

Robine J-M, Cheung SLK, Le Roy S, Van Oyen H, Griffiths C, Michel J-P, Herrmann FR (2008) Death toll exceeded 70,000 in Europe during the summer of 2003. Comptes Rendus Biol 331:171–178

Saha S, Moorthi S, Pan H-L, Wu X, Wang J, Nadiga S, Tripp P, Kistler R, Woollen J, Behringer D (2010) The NCEP climate forecast system reanalysis. Bull Am Meteorol Soc 91:1015–1057

Sillmann J, Croci-Maspoli M (2009) Present and future atmospheric blocking and its impact on European mean and extreme climate. Geophys Res Lett 36:L10702

Simister J, Cooper C (2005) Thermal stress in the USA: Effects on violence and on employee behaviour. Stress Health 21:3–15

Wang L, Chen W (2010) How well do existing indices measure the strength of the East Asian winter monsoon? Adv Atmos Sci 27:855–870

Wang B, Lin HO (2002) Rainy season of the Asian–Pacific summer monsoon. J Clim 15:386–378

Wang B, Zhang Y, Lu M (2004) Definition of South China Sea monsoon onset and commencement of the East Asia summer monsoon. J Clim 17:699–710

Wang L, Huang R, Gu L, Chen W, Kang L (2009) Interdecadal variations of the East Asian winter monsoon and their association with quasi-stationary planetary wave activity. J Clim 22:4860–4872

Wang W, Zhou W, Wang X, Fong SK, Leong KC (2013) Summer high temperature extremes in Southeast China associated with the East Asian jet stream and circumglobal teleconnection. J Geophys Res Atmos 118:8306–8319

Wang W, Zhou W, Chen D (2014) Summer high temperature extremes in southeast China: Bonding with the El Niño–Southern Oscillation and East asian summer monsoon coupled system. J Clim 27:4122–4138

Wang W, Zhou W, Li X, Wang X, Wang D (2016) Synoptic-scale characteristics and atmospheric controls of summer heat waves in China. Clim Dyn 46:2923–2941

Webster PJ, Yang S (1992) Monsoon and ENSO: Selectively interactive systems. Q J R Meteorol Soc 118:877–926

White CJ, Hudson D, Alves O (2014) ENSO, the IOD and the intraseasonal prediction of heat extremes across Australia using POAMA-2. Clim Dyn 43:1791–1810

Xie P, Chen M, Yang S, Yatagai A, Hayasaka T, Fukushima Y, Liu C (2007) A gauge-based analysis of daily precipitation over East Asia. J Hydrometeorol 8:607–626

Xu J, Deng Z, Chen M (2009) A summary of studying on characteristics of high temperatureand heat wave damage in China (in Chinese). J Arid Meteorol 27:163–167

You Q, Jiang Z, Kong L, Wu Z, Bao Y, Kang S, Pepin N (2017) A comparison of heat wave climatologies and trends in China based on multiple definitions. Clim Dyn 48:3975–3989

Zhang Y, Li T, Wang B, Wu G (2002) Onset of the summer monsoon over the indochina peninsula: climatology and interannual variations. J Clim 15:3206–3221

Zhang Z, Chan JC, Ding Y (2004) Characteristics, evolution and mechanisms of the summer monsoon onset over Southeast Asia. Int J Climatol 24:1461–1482

Zuo J, Pullen S, Palmer J, Bennetts H, Chileshe N, Ma T (2015) Impacts of heat waves and corresponding measures: a review. J Clean Prod 92:1–12

Terms and Conditions

Springer Nature journal content, brought to you courtesy of Springer Nature Customer Service Center GmbH (“Springer Nature”).
Springer Nature supports a reasonable amount of sharing of research papers by authors, subscribers and authorised users (“Users”), for small-scale personal, non-commercial use provided that all copyright, trade and service marks and other proprietary notices are maintained. By accessing, sharing, receiving or otherwise using the Springer Nature journal content you agree to these terms of use (“Terms”). For these purposes, Springer Nature considers academic use (by researchers and students) to be non-commercial.
These Terms are supplementary and will apply in addition to any applicable website terms and conditions, a relevant site licence or a personal subscription. These Terms will prevail over any conflict or ambiguity with regards to the relevant terms, a site licence or a personal subscription (to the extent of the conflict or ambiguity only). For Creative Commons-licensed articles, the terms of the Creative Commons license used will apply.
We collect and use personal data to provide access to the Springer Nature journal content. We may also use these personal data internally within ResearchGate and Springer Nature and as agreed share it, in an anonymised way, for purposes of tracking, analysis and reporting. We will not otherwise disclose your personal data outside the ResearchGate or the Springer Nature group of companies unless we have your permission as detailed in the Privacy Policy.
While Users may use the Springer Nature journal content for small scale, personal non-commercial use, it is important to note that Users may not:

1. use such content for the purpose of providing other users with access on a regular or large scale basis or as a means to circumvent access control;
2. use such content where to do so would be considered a criminal or statutory offence in any jurisdiction, or gives rise to civil liability, or is otherwise unlawful;
3. falsely or misleadingly imply or suggest endorsement, approval , sponsorship, or association unless explicitly agreed to by Springer Nature in writing;
4. use bots or other automated methods to access the content or redirect messages
5. override any security feature or exclusionary protocol; or
6. share the content in order to create substitute for Springer Nature products or services or a systematic database of Springer Nature journal content.

In line with the restriction against commercial use, Springer Nature does not permit the creation of a product or service that creates revenue, royalties, rent or income from our content or its inclusion as part of a paid for service or for other commercial gain. Springer Nature journal content cannot be used for inter-library loans and librarians may not upload Springer Nature journal content on a large scale into their, or any other, institutional repository.
These terms of use are reviewed regularly and may be amended at any time. Springer Nature is not obligated to publish any information or content on this website and may remove it or features or functionality at our sole discretion, at any time with or without notice. Springer Nature may revoke this licence to you at any time and remove access to any copies of the Springer Nature journal content which have been saved.
To the fullest extent permitted by law, Springer Nature makes no warranties, representations or guarantees to Users, either express or implied with respect to the Springer nature journal content and all parties disclaim and waive any implied warranties or warranties imposed by law, including merchantability or fitness for any particular purpose.
Please note that these rights do not automatically extend to content, data or other material published by Springer Nature that may be licensed from third parties.
If you would like to use or distribute our Springer Nature journal content to a wider audience or on a regular basis or in any other manner not expressly permitted by these Terms, please contact Springer Nature at

onlineservice@springernature.com